IUTAM Symposium on 50 Years of Chaos : Applied and Theoretical
Kyoto, Japan, November 28 - December 2, 2011

Chaotic Dynamics of Impact Oscillator with SMA Constraint

Ekaterina Pavlovskaia[1], Elena Sitnikova[1], James Ing[1], Marian Wiercigroch[1]
[1] *Centre for Applied Dynamics Research, School of Engineering, Aberdeen University, King's College, Aberdeen, AB24 3UE, Scotland, UK, e.pavlovskaia@abdn.ac.uk*

In this paper chaotic dynamics of impact oscillator with one sided motion constraint made of a shape memory alloy (SMA) will be discussed [1,2]. The system was modelled using the thermo-mechanical description of the SMA element which follows the formulation proposed by Bernardini et. al. [3,4]. The thermo-mechanical coupling terms, which are included in the energy balance equation, allow to undertake the non-isothermal analysis.

Physical model and equations of motion

The dynamical system under consideration is the one degree-of-freedom piecewise smooth oscillator shown in Fig. 1a. The system consists of a mass m supported by a primary spring of stiffness K_1 and a damper μ. The oscillating mass collides with a motion restraint made of SMA having pseudoelastic behaviour. The gap between the mass and the SMA constraint in the equilibrium position is g. The external force in the form of harmonic excitation $F = A\cos(\Omega)$ is applied to the base of the oscillator. The considered system has two types of nonlinearities. The first one is associated with the discontinuous characteristics caused by intermittent contacts, whereas the second type of nonlinearity is related to the pseudoelastic nature of the SMA element. In order to examine the influence of the SMA on the dynamic response of such system, a comparison with equivalent oscillator with a plain elastic secondary support has been made.

The equations of motion for the pseudoelastic oscillator were derived in [1,2] and they are as follows:

$$\begin{aligned}
\dot{x} &= v,\\
\dot{v} &= -\frac{K_1}{m}x - \frac{\mu}{m}v - \frac{K}{m}(x + g - \delta\xi\,\mathrm{sign}(x+g))\mathsf{H}(-x-g) + \frac{A\Omega^2}{m}\cos(\Omega t),\\
\dot{\xi} &= \mathcal{H}(\xi,\xi_0)\left[Kv\,\mathrm{sign}(x) - \frac{bh(\theta_e-\theta)}{c}\right]\mathsf{H}(-x-g),\\
\dot{\theta} &= \left[\frac{\Lambda(\xi,\xi_0)+b\delta\theta}{c}\right]\dot{\xi}\,\mathsf{H}(-x-g) + \frac{h(\theta_e-\theta)}{c},
\end{aligned} \tag{1}$$

Here x is the mass displacement, θ is the temperature of the SMA element and ξ is a state variable called volume fraction of martensite introduced to describe the phase transformation evolution, and all other parameters and functions are defined in [2]. $\xi \in [0,1]$ and zero value corresponds to SMA material being fully in the austenite phase and the one value corresponds to material being fully in martensite state.

Numerical and Experimental Results

The experimental investigations were carried out on the impact oscillator shown in Fig. 1b which consists of a block of mild steel supported by parallel leaf springs providing the primary stiffness and preventing the mass from rotation. The secondary stiffness comprised of a stiff steel beam with a hinge supported by pseudoelastic

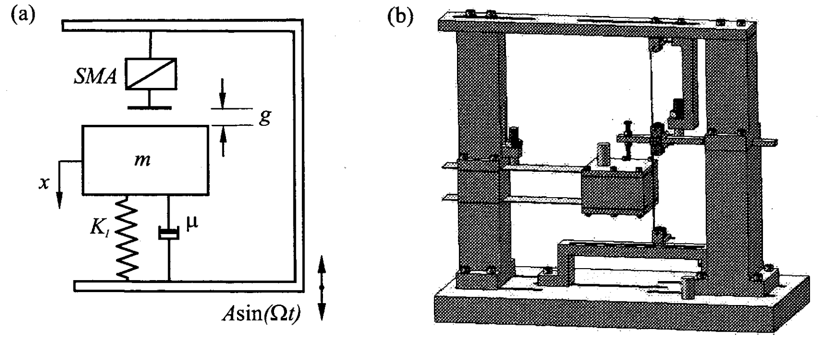

Figure 1: (a) Physical model of impact oscillator with SMA constraint [2]; (b) schematic of the impact oscillator where the secondary constraint is comprised of a stiff steel beam with a hinge supported by pseudoelastic wires.

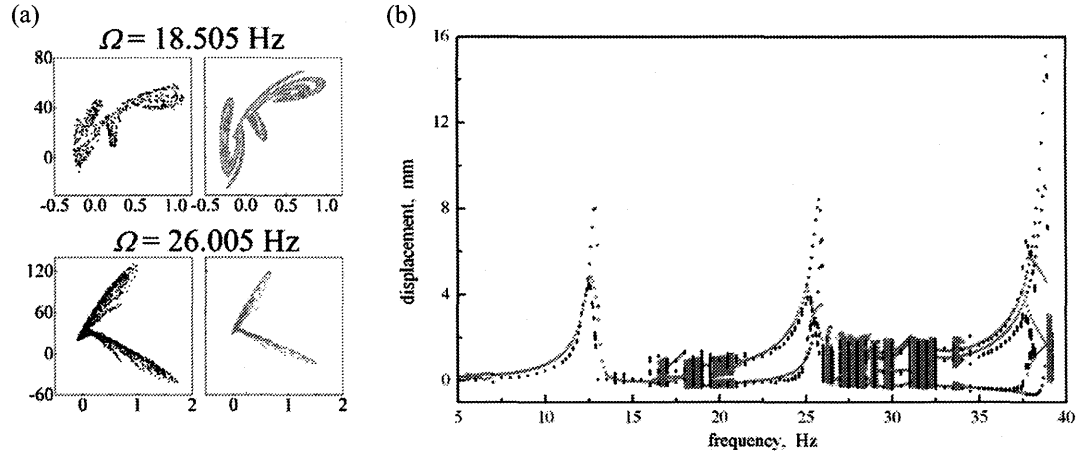

Figure 2: (a) Chaotic attractors recorded experimentally (in black) and calculated numerically (in red); (b) comparison of the experimentally recorded bifurcation diagram (black) for pseudoelastic oscillator with numerically calculated diagram for pseudoelastic oscillator (orange) and numerically calculated for elastic oscillator (blue).

wires is mounted on a separate column. Contact between the mass and the beam is made when their relative displacement is equal to zero. In practice, the contact is through a bolt which is attached to the beam. The oscillator rig was mounted on an electro-dynamic shaker which provided the harmonic excitation through the base. Displacement of the oscillator was measured with an eddy current probe displacement transducer attached to the upper leaf spring. The acceleration of the oscillator was measured using an accelerometer mounted directly on the mass. The signals from these two devices were observed in real time using the data acquisition system. A Savitzky-Golay algorithm was used to smooth the data, where a second order polynomial fitted to the eight surrounding data points gave the best results. As can been seen from the Fig. 2a the good correspondence between the experimental and numerical results has been obtained.

Our numerical study of the impact oscillator shows that the damping effect of the SMA can be very significant. The experimentally obtained bifurcation diagram under varying excitation frequency ω is shown in Fig. 2b in black together with numerically obtained diagram (in orange) and the diagram obtained for for elastic oscillator (in blue). As can be seen, a large variety of periodic and chaotic responses are observed in both cases, and there are several regions where the bifurcation diagrams coincide. This means that in these regions the intensity of the impact force acting on the SMA constraint is not high enough to initiate the phase transformations, and therefore the SMA element acts as a linear spring. It appeared that the experimental displacement amplitudes at resonant peaks were nearly half the size of the numerically calculated for the elastic oscillator, and the vibration reduction was larger at higher forcing frequency.

Conclusions

The conducted numerical investigations suggest that the system can exhibit complex dynamic responses, which if appropriately controlled can be used for vibration reduction. A comparison with an equivalent elastic oscillator is made and it is found that the low amplitude regimes are not affected by the SMA element. On the contrary, for the large amplitude responses, a significant vibration reduction is achieved due to the phase transformation hysteresis loop. Various bifurcation scenarios are constructed and the influence of the SMA element is discussed. To verify the obtained theoretical predictions, an experimental rig was designed and the experimental studies have been carried out. The results indicate that in some frequency ranges the vibration reduction can be achieved and they corroborate well with the numerics.

References

[1] Sitnikova, E., Pavlovskaia, E.E. and Wiercigroch, M. (2008) Dynamics of an impact oscillator with SMA constraint, *European Physical Journal - Special Topics* **165**(1):229-238.

[2] Sitnikova, E., Pavlovskaia, E.E., Wiercigroch, M. and Savi, M.A. (2010) Vibration reduction of the impact system by an SMA restraint: Numerical studies, *International Journal of Nonlinear Mechanics* **54**:837-849.

[3] Bernardini, D., Pence, T. (2002) Models for one-variant shape memory materials based on dissipation functions, *International Journal of Non-Linear Mechanics* **37**:1299-1317.

[4] Bernardini, D., Rega, G. (2005) Thermomechanical modelling, nonlinear dynamics and chaos in shape memory oscillators, *Mathematical and Computer Modelling of Dynamical Systems* **11**(3):291-314.